

Substrate Integrated Waveguide Cavity Backed Wideband Slot Antenna for 5G Applications

Amit KUMAR¹, Munish KUMAR², Amit Kumar SINGH¹

¹ Department of Electronics Engineering, Indian Institute of Technology (BHU), Varanasi, India

² USIC&T, Guru Gobind singh Indraprastha University, Dwarka New Delhi, India

amitk.rs.ece17@iitbhu.ac.in

Submitted October 5, 2020 / Accepted March 19, 2021

Abstract. *In this article, a study of wideband substrate integrated waveguide (SIW) cavity based slot antenna is presented. The proposed antenna consists of a U-shaped slot etched in the ground plane which helps in achieving the wideband behaviour. A detailed analysis of the SIW cavity and prediction of various modes propagating inside it using accurate design equations are discussed. An equivalent circuit modeling of the proposed antenna along with surface current distributions at various resonating frequencies is also performed. Parametric study on various parameters to improve the performance in terms of wide impedance bandwidth, gain and efficiency levels are also discussed in detail. The fabricated prototype of the proposed SIW antenna shows the reflection coefficient $|S_{11}| \leq 10$ dB in frequency range from 26.20–30.30 GHz (14.51%) which are in good agreement with the simulated results. A peak gain and maximum radiation efficiency of 7.65 dBi and 91.29%, respectively. A low variation in peak gain (± 0.26 dBi) and radiation efficiency ($\pm 0.09\%$) within the operating frequency range is seen. A good matching characteristics along with good level of gain, radiation efficiency levels and stable radiation patterns makes the proposed antenna a suitable candidate for 5G applications.*

Keywords

5G applications, cavity-backed slotted antenna, substrate integrated waveguide (SIW), wideband

1. Introduction

The fifth-generation (5G) is a mobile technology in order to meet the high data rate requirements, high bandwidth, improved security with shorter latency in coming years over 4G systems. The technologies under 5G development include massive multiple-input-multiple-output (MIMO), ultra-dense networking, dynamic spectrum sharing and full digital or hybrid beamforming [1], [2]. It has been decided in World Radiocommunication Conference 2015 that

operation of terrestrial International Mobile Telecommunications (IMT) services will take place within the frequency range between 24.25 to 86 GHz [3]. In this regard, 28 GHz frequency band (millimeter wave) has become a prominent candidate supporting high-speed communications (data rates up to 10 Gbps) along with large available bandwidth [4], [5] and useful for non-line-of-sight communications.

Low-profile microstrip patch antennas (MSPAs) are becoming popular and receiving great research interests due to their compact size, ease in fabrication features. However, their performance is inherently suffered from issues including low gain and narrow bandwidth (typically few percentages only). One way to overcome these issues is to use substrate integrated waveguide (SIW) technology which combines planar circuits and non-planar waveguide circuits in a common substrate [6]. At higher frequencies, an extremely high tolerance is required in manufacturing MSPAs which is not very efficient. Hence, waveguide is preferred over simple patch antennas. A simple SIW antenna structure comprises of at least one radiating element as a first metal layer, a ground plane as a second metal layer, a dielectric substrate material positioned between these metallic layers and an electric wall arrangement. This electric wall arrangement consists of two (or more) rows of vias drilled inside the substrate and then filled with metal parallel to each other which resembles the waveguide arrangement [7]. With proper tuning of diameter of the metalized vias drilled and gap among them, the leakage current flowing out of the waveguide and hence the radiation losses can be minimized. Numerous advantages of SIW structures such as (a) low-cost fabrication, (b) high quality factor due to better suppression of surface waves [8], (c) reduced coupling and wider scan performance in array environment [9] and (d) easy integration of active and passive elements on the same substrate along with the radiating antenna (system-on-substrate, SoS), thereby reducing the losses and parasitics [10–12]. Recently, several wideband antenna structures have been proposed in the literature using SIW cavity backed antennas. A multilayered SIW MIMO antenna with high-isolation with dumbbell shaped slot is discussed in [13] shows impedance bandwidth of 21.90% (11.80–14.60 GHz). SIW technology can also be used in enhancing the bandwidth in

MSPA arrays. In [8], an array of 2×2 , 4×4 and 8×8 antenna elements for enhancing bandwidth is discussed. A SIW-interated dielectric resonator (DRA) based antenna as discussed in [14] shows bandwidth of 3.30 GHz ranging from 35.60–38.90 GHz. Another SIW based triangular ring slotted antenna has been presented in [15] which exhibits bandwidth of 13.53% (14.43–16.49 GHz) and suitable for K_u -band applications. Similar to this, a SIW based antenna with triangular shaped complementary split ring shaped slot is discussed in [16] for 5G applications and shows bandwidth of 16.67% centered around 28 GHz frequency band. Various microwave components such as 4-port directional coupler [17], 6-port directional coupler [18] and magic Tee [19] can also designed using SIW technology. In this paper, the authors have designed an inset-fed rectangular MSPA SIW antenna to operated at 28 GHz frequency band for 5G wireless communication systems. This rectangular patch antenna is drilled with arrays of metallic vias on its three sides thereby forming PEC walls and fourth side as PMC wall being devoid of any metallic via. All the simulations are performed using ANSYS Electronics Desktop ver. 18.0.

2. Design of the Proposed Antenna

2.1 Total Antenna Configuration

The configuration of the proposed antenna (both top and bottom view) is outlined in Fig. 1 which consists of an inset-fed rectangular patch antenna, an U-shaped slot in the ground plane and a SIW cavity created by the single row of the metallic cylindrical vias around the rectangular patch and inside the planar substrate thereby making the four side-walls of the cavity. In Fig. 1, the metallic (or copper) part of the proposed antenna are represented with yellow, substrate with light green and metallic vias with blue color. These metallic vias connect the ground plane and radiating patch with each other. The proposed antenna is designed on Rogers RT/Duroid 5880 substrate having permittivity $\epsilon_r = 2.2$ and thickness $h = 0.508$ mm with extremely low loss tangent $\tan \delta = 0.0009$. Many closely and equally spaced cylindrical metallic vias are drilled into the substrate and metalized from inside, thus acting as a short between the rectangular patch and ground plane. The propagation of electromagnetic waves inside this SIW cavity resembles the propagation in artificial periodic waveguide thereby minimizing the leakage losses to adequate levels. If the vias are placed in such a way that they cut the flow of currents, then a large amount of radiation may appear. On the other hand, if the vias are placed in the direction of the current, then only a little or no radiation will take place. The presence of gaps between the vias does not allow the TM modes to exist within the SIW [20]. The overall physical dimensions of the proposed antenna are 18×14 mm². The detailed optimized dimension of the proposed SIW antenna are: $L_{\text{gnd}} = 18$ mm, $W_{\text{gnd}} = 14$ mm, $L_{\text{SIW}} = 6$ mm, $W_{\text{SIW}} = 9$ mm, $d_{\text{via}} = 0.4$ mm, $p_{\text{via}} = 0.6$ mm, $w_{\text{feed}} = 3.37$ mm, $L_{\text{feed}} = 8$ mm, $y_{\text{in}} = 5.5$ mm, $x = 1.68$ mm, $l_{\text{sy}} = 4.1$ mm, $l_{\text{sx}} = 5$ mm, $w_s = 1$ mm.

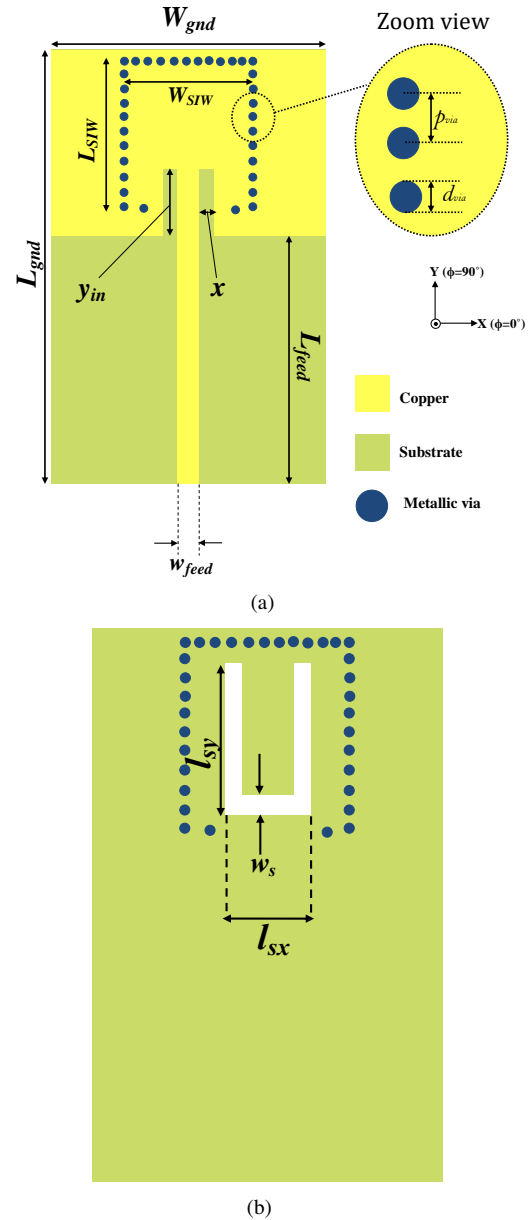


Fig. 1. The geometrical configuration of the proposed antenna. (a) Top view; (b) Bottom view.

2.2 Design Guidelines

2.2.1 SIW Cavity

The main purpose of using the metalized vias forming the SIW cavity is to effectively suppress and effects of edge diffraction of surface waves propagating over the entire substrate and confine the energy beneath the radiating patch. In this way, this array of metalized vias will also improve the radiation performance (gain and directivity levels). For this, the via diameter should be large and the distance between the vias is kept as small as possible in order to minimize the leakage loss ($L_{\text{leakage}} = -10 \log[S_{11}^2 + S_{12}^2]$) between the adjacent vias [21]. The center-to-center distance between each via of diameter d_{via} is represented by p_{via} .

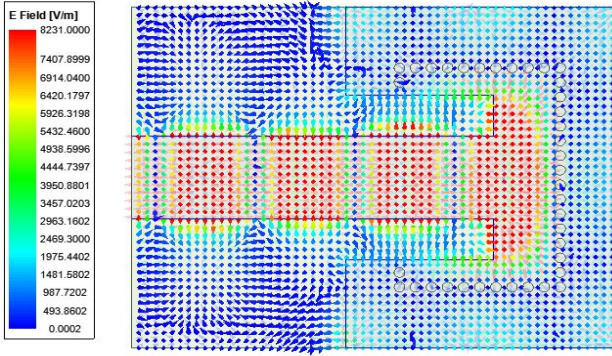


Fig. 2. E-field distribution inside the SIW cavity.

Two conditions related to these two parameters for minimizing the radiation loss are given by [22]:

$$\frac{p_{\text{via}}}{d_{\text{via}}} < 2, \tag{1a}$$

$$d_{\text{via}} < \frac{\lambda_g}{5}. \tag{1b}$$

The term W_{SIW} is the distance between the centers of two vias of opposite rows as shown in Fig. 1(a) and

$$\lambda_g = \frac{2}{\sqrt{4f^2\epsilon_r - \left(\frac{1}{W_{\text{RWG}}}\right)^2}} \tag{2}$$

for dominant TE₁₀ mode [23] is the guided wavelength corresponding to highest wavelength or lowest resonant frequency for 5G applications (which is around 26 GHz). Equations (1a) and (1b) ensure in keeping the leakage loss at negligible level. A rough estimate of cavity dimensions W_{SIW} and L_{SIW} (both are in millimeter) for a wideband antenna of bandwidth equals to $(f_H - f_L)$ (both are in GHz) can be calculated by [16]:

$$L_{\text{SIW}} \approx \frac{580.95}{\sqrt{\epsilon_r}} \sqrt{\frac{1}{4f_H^2 - f_L^2}}, \tag{3a}$$

$$W_{\text{SIW}} \approx \frac{580.95}{\sqrt{\epsilon_r}} \sqrt{\frac{1}{4f_L^2 - f_H^2}}. \tag{3b}$$

To cover the high frequency band of 5G completely, the upper (f_H) and lower (f_L) cutoff frequencies are taken as 26 GHz and 30 GHz, respectively. The relationship between the resonance frequency for any TE_{mnp} of the SIW cavity formed by the vias and geometrical parameters related to the proposed antenna dimensions can be given by following equation [12]:

$$f_{mnp} = \frac{1}{2\sqrt{\mu_0\epsilon_0}} \sqrt{\left(\frac{m}{L_{\text{RWG}}}\right)^2 + \left(\frac{n}{W_{\text{RWG}}}\right)^2 + \left(\frac{p}{h}\right)^2} \tag{4}$$

where $L_{\text{RWG}} = L_{\text{SIW}} - \frac{1.08p_{\text{via}}^2}{d_{\text{via}}} + \frac{0.1p_{\text{via}}^2}{L_{\text{SIW}}}$, (5a)

$$W_{\text{RWG}} = W_{\text{SIW}} - \frac{1.08p_{\text{via}}^2}{d_{\text{via}}} + \frac{0.1p_{\text{via}}^2}{W_{\text{SIW}}}. \tag{5b}$$

The terms m, n, p are the modal indices, L_{RWG} and W_{RWG} are the effective lengths and widths of the SIW cavity (equivalent to the rectangular waveguide), respectively. For obtaining more accurate values of L_{RWG} and W_{RWG} , following expressions can be considered:

$$W_{\text{RWG}} = W_{\text{SIW}} \left(\zeta_1 + \frac{\zeta_2}{\frac{p_{\text{via}}}{d_{\text{via}}} + \frac{\zeta_1 + \zeta_2 - \zeta_3}{\zeta_3 - \zeta_1}} \right), \tag{6a}$$

$$\zeta_1 = 1.0198 + \frac{0.3465}{\frac{W_{\text{SIW}}}{p_{\text{via}}} - 1.0684}, \tag{6b}$$

$$\zeta_2 = -0.1183 - \frac{1.2729}{\frac{W_{\text{SIW}}}{p_{\text{via}}} - 1.2010}, \tag{6c}$$

$$\zeta_3 = 1.0082 - \frac{0.9163}{\frac{W_{\text{SIW}}}{p_{\text{via}}} + 0.2152}. \tag{6d}$$

For $W_{\text{SIW}}=9$ mm, $p_{\text{via}}=0.6$ mm and $d_{\text{via}}=0.4$ mm, the values of $\zeta_1, \zeta_2, \zeta_3$ and W_{RWG} will be 1.05, -0.21, 0.95 and 8.69, respectively. Replacing W_{RWG} by L_{RWG} in equation (6a) gives L_{RWG} equals to 5.80 mm. The E-field distribution of the SIW cavity is shown in Fig. 2.

2.2.2 Patch Antenna and U-shaped Slot

Apart from the SIW cavity, the inset-fed MSPA can be designed using the following equations:

$$W_{\text{patch}} (= W_{\text{gnd}}) = \frac{c}{2f_r \sqrt{\frac{\epsilon_r + 1}{2}}}, \tag{7a}$$

$$L_{\text{patch}} (= L_{\text{gnd}} - L_{\text{feed}}) = \frac{c}{2f_r \sqrt{\epsilon_{\text{eff}}}} - 2\Delta L \tag{7b}$$

where

$$\epsilon_{\text{eff}} = \frac{\epsilon_r + 1}{2} + \frac{\epsilon_r - 1}{2\sqrt{1 + 12\frac{h}{W_{\text{patch}}}}}$$

and

$$\Delta L = 0.412h \frac{(\epsilon_{\text{eff}} + 0.3)\left(\frac{W_{\text{patch}}}{h} + 0.264\right)}{(\epsilon_{\text{eff}} - 0.258)\left(\frac{W_{\text{patch}}}{h} + 0.8\right)}.$$

It is necessary to set the U-shaped slot dimensions at half-wavelength so as to get better radiation performance, i.e., gain and radiation efficiency levels. The relationship between the length of the slot and resonating frequency is given by:

$$f_{r,\text{slot}} \approx \frac{c}{2(2l_{\text{sy}} + l_{\text{sx}} - w_s)}. \tag{8}$$

It is clear from Fig. 3 that current density is maximum around the U-shaped slot at the resonating frequency.

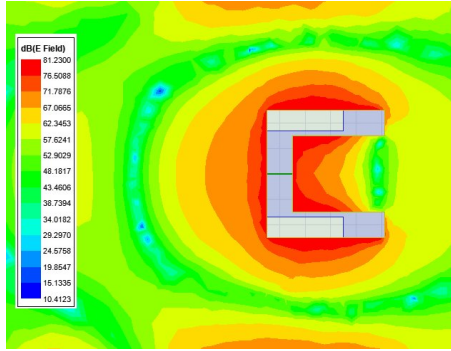


Fig. 3. Surface current density around the U-shaped slot at $f_{r,slot}=28$ GHz.

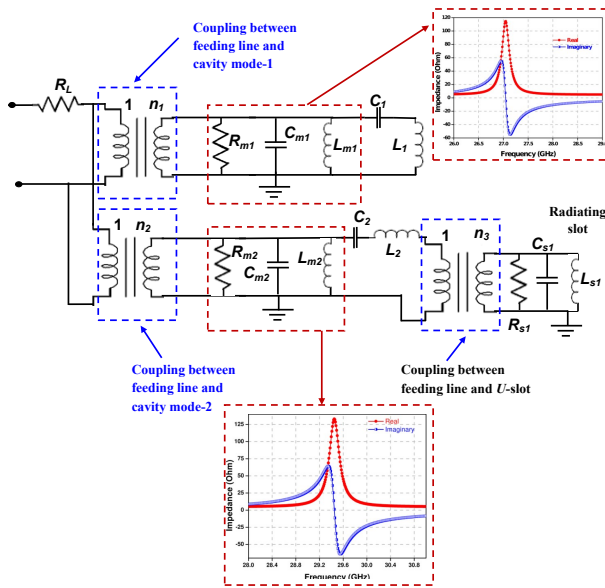


Fig. 4. Final equivalent circuit of the proposed SIW antenna.

3. Equivalent Circuit Analysis

The equivalent circuit of the proposed SIW antenna (while ignoring the material losses) is shown in Fig. 4. Here, the presence of periodic vias decreases the overall permittivity of the substrate material used and hence suppresses the standing waves resulting into propagation of electromagnetic waves more the the free space. To analyze the propagating modes inside the SIW cavity and their coupling/interaction with the U-shaped slot, equivalent circuit for the proposed antenna is designed and discussed.

1. The equivalent circuit of the proposed antenna mainly consists of three branches which shows coupling of feed-line with mode-1, mode-2 and U-shaped slot.
2. Here, the SIW cavity can be modeled as a parallel combination of RLC resonant circuit. The coupling between the feed-line and the propagating modes is represented with the help of an ideal transformer with turns-ratio 1 : n . The optimized values of the circuit elements are as follows: $R_L = 4.68 \Omega$, $n_1 = 25$,

$$R_{m1} = 80.26 \text{ k}\Omega, C_{m1} = 11 \text{ fF}, L_{m1} = 3.148 \text{ nH}, \\ R_{m2} = 80.26 \text{ k}\Omega, L_{m2} = 2.98 \text{ nH}, C_{m2} = 9.8 \text{ fF} \text{ and } n_2 = 27.$$

3. In order to widen the impedance bandwidth, U-shaped slot is etched in the ground plane of the proposed SIW antenna. The final equivalent circuit of the proposed SIW antenna considering both the propagating modes is shown in Fig. 4. Here, the combination of (R_{m1} , L_{m1} and C_{m1}) and (R_{m2} , L_{m2} and C_{m2}) corresponds to the cavity resonators which are coupled with the slot antenna with the help of transformers having turns-ratio n_1 and n_2 , respectively. To model the effect of loading between two different cavity modes, a Tee network consisting of a series combination of a capacitor (C_1 or C_2) and an inductor (L_1 or L_2) is also placed with each arm. This capacitor-inductor series combination offer high impedance at the resonant frequencies and hence, a very small amount of signal is allowed to pass through them.

4. Parametric Analysis

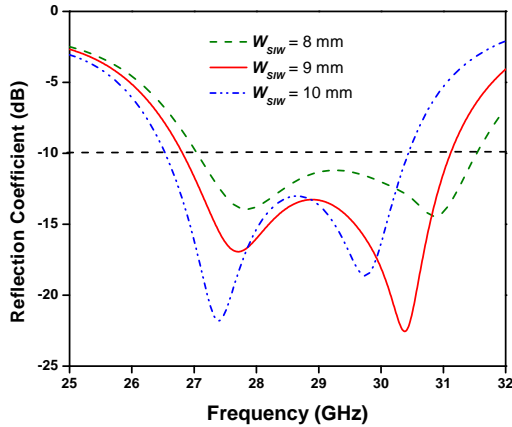
In order to obtain the desired resonant frequency and matching characteristics over a specific range of frequency, parameterization over various parameters has been performed. While varying a particular parameter, the all other parameters are kept constant. In this section, the effect of parameters namely SIW cavity width, i.e., center-to-center distance between the rows of the metallic vias and arm length of U-shaped slot has been studied. All the simulations related to parametric analysis have been performed using optimetrics option given in the ANSYS Electronics Desktop version 18.0.

4.1 Influence of Cavity Width W_{SIW}

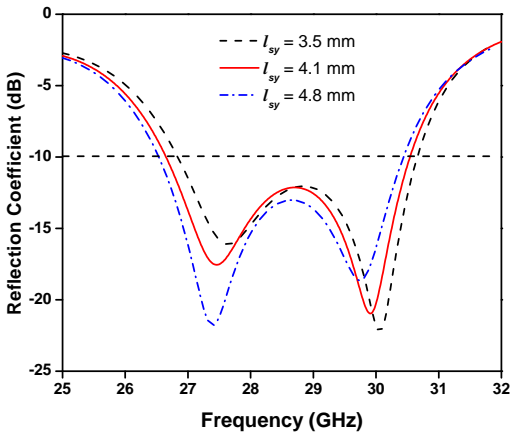
It is evident from equation (4) that any variation in the width of the SIW cavity brings variation in its resonating frequency. Fig. 5(a) shows the variation in matching characteristics with change in W_{SIW} . As W_{SIW} varies from 8 mm to 10 mm, the upper cutoff frequency changes from 31.54 GHz to 30.44 GHz, i.e., by 3.49%. A very little or no effect on lower resonating frequency has been noticed.

4.2 Influence of Arm Lengths of U Slot

Though the W_{SIW} primarily determines the operating frequency of the antenna, however it can be modeled l_{sy} up to some extent. The presence of U-shaped slot in the ground plane decreases the quality factor and hence helps in improving the impedance bandwidth of the proposed SIW antenna. The effect of slot arm length l_{sy} is shown in Fig. 5(b). As the length l_{sy} increases, a longer effective current flows on the bottom surface of the cavity which reduces the resonating frequency (inverse relation). When the slot and cavity dimensions are in resonance, the energy will radiate into the space with utmost extent.



(a)



(b)

Fig. 5. Variation in reflection coefficient (S_{11}) while varying (a) cavity width W_{SIW} and (b) arm lengths of U-shaped slot.

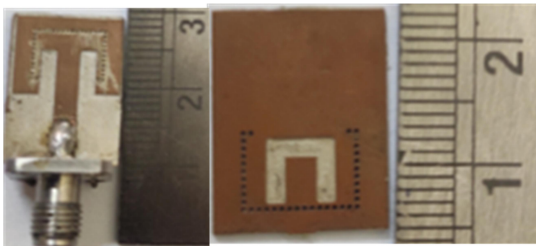


Fig. 6. Photograph of the proposed antenna fabricated prototype.

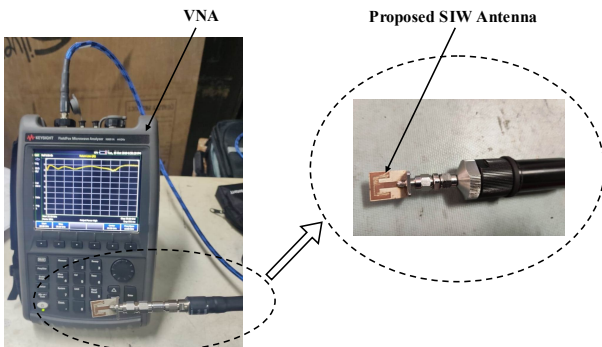


Fig. 7. Testing of the proposed SIW antenna for measuring reflection coefficient using VNA.

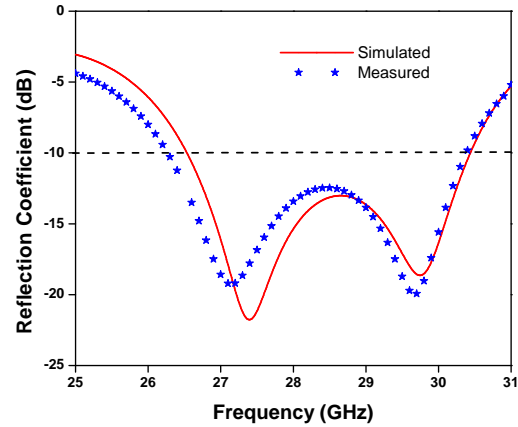


Fig. 8. Simulated (solid red line) and measured (blue dotted line) reflection coefficient of the proposed antenna.

5. Results and Discussion

5.1 Matching Characteristics

Figure 6 shows the fabricated prototypes of the proposed SIW antenna having U-shaped slot in the ground plane. The proposed antenna is fabricated using standard PCB process and process of making vias inside the substrate material is explained in detail in [24]. The measurement of reflection coefficient (S_{11}) can be accomplished by using the Keysight N9951A FieldFox Microwave Analyzer as shown in Fig. 7. A 2.92 mm(F) 4-hole panel mount 50Ω connector (can work up to 40 GHz) is connected to the proposed antenna for measurement purpose. Figure 8 shows the simulated and measured S_{11} for the proposed antenna having an impedance bandwidth of 14.51% (26.20–30.30 GHz) for $|S_{11}| \leq -10$ dB. A little deviation at lower frequency side is noticed which may be due to permittivity fluctuations, fabrication errors and soldering with connector. Hence, the proposed antenna is best suited for 5G application including 27.50–28.28 GHz in Japan, 26.50–29.50 GHz in Korea and 27.50–28.35 GHz in USA.

5.2 Radiation Characteristics

All the measurement related to gain and efficiency are performed within the anechoic chamber as shown in Fig. 9. Figure 10 shows the measured gain and radiation efficiency of the proposed antenna structure and a simple inset-fed antenna, i.e., without any SIW cavity and slot, respectively. It is clear that the presence of the SIW cavity and slot improves both gain and efficiency levels by minimizing the losses as compared to a simple MSPA having none of them. A maximum gain of 7.65 dBi at 28.5 GHz is obtained with variation less than ± 0.26 dBi within the operating frequency range. Also, the radiation efficiency of the proposed antenna is always larger than 90% with maximum of 91.29% at 28.5 GHz and variation less than $\pm 0.09\%$ within the operating frequency range. The 1-dB gain bandwidth of the

Reference/Year	Dimensions (mm ³)	Bandwidth (%)	Peak Gain (dBi)	Technology used
[25]/2020	30×35×0.76	25.50–29.60 GHz (14.88%)	8.3	Defected ground structure (DGS) MIMO
[26]/2019	38.58×38.58×0.762	27–29.20 GHz (7.83%)	12	Bow-tie antenna with DGS
[27]/2020	-	27.50–28.35 GHz (3.04%)	11	Rotated wide-slot
[28]/2018	11×31×0.254	26–31 GHz (17.54%)	10	Metamaterial based
[29]/2018	-	24.50–26.50 GHz (7.84%)	≥6	Aperture-fed + reconfigurable
[30]/2020	45×36×(0.787+0.65)	27.90–28.50 GHz (2.13%)	6.8	Multilayer configuration
Proposed Work	18×14×0.508	26.20–30.30 GHz (14.51%)	7.65	SIW

Tab. 1. Comparison of measured results of the proposed slotted SIW antenna with antennas proposed for 5G applications.

proposed antenna is 11.93% (26.80–30.20 GHz) and radiation efficiency within this range is larger than 90% which is about 8% better than the slotted SIW antenna reported in [31].

The simulated and measured radiation patterns in XZ-plane (or $\phi = 0^\circ$) and YZ-plane (or $\phi = 90^\circ$) are illustrated in Fig. 11. The isolation level in XZ-plane and YZ-plane is about 28 dB and 35.4 dB, respectively at 27.1 GHz whereas the isolation level in XZ-plane and YZ-plane is less than 30 dB and 38 dB, respectively at 29.6 GHz. The mismatch between the simulation results and measurement results can be observed due to the misalignment between the fabricated proposed SIW antenna and the horn antenna (of known gain) inside the anechoic chamber while performing the measurement. A comparison of the proposed antenna with the already proposed antenna structures is given in Tab. 1.



Fig. 9. Proposed antenna placed inside anechoic chamber for the measurement of gain and radiation patterns.

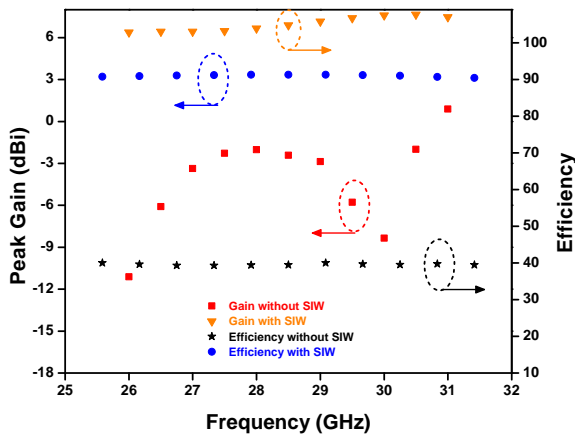


Fig. 10. Gain and efficiency of the proposed antenna (without SIW cavity and slot).

6. Conclusion

A wideband SIW cavity-backed slotted antenna is proposed and discussed in this paper. The U-shaped slot is used to perturb the field distribution of the SIW cavity and helps in achieving a wideband response. The proposed antenna in presence of SIW cavity and U-shaped slot together shows impedance bandwidth of about 14.50% ranging from 26.20–30.30 GHz along with maximum peak gain and efficiency of 7.65 dBi and 91.29%, respectively. As compared to the conventional counterpart having no cavity and slot, the proposed antenna shows better gain and efficiency average levels by 11.09 dBi and 51.42%, respectively within the operating frequency range. The parametric study of cavity and slot dimensions reveals their effect on antenna matching and resonance characteristics. The measured results of the proposed fabricated antenna prototype are in concordance with the simulated proposed antenna design. Due to its simple structure, high gain/efficiency levels and good radiation patterns, the proposed antenna can be an alternative for 5G and other wireless applications (including 27.50–28.28 GHz in Japan, 26.50–29.50 GHz in Korea and 27.50–28.35 GHz in USA).

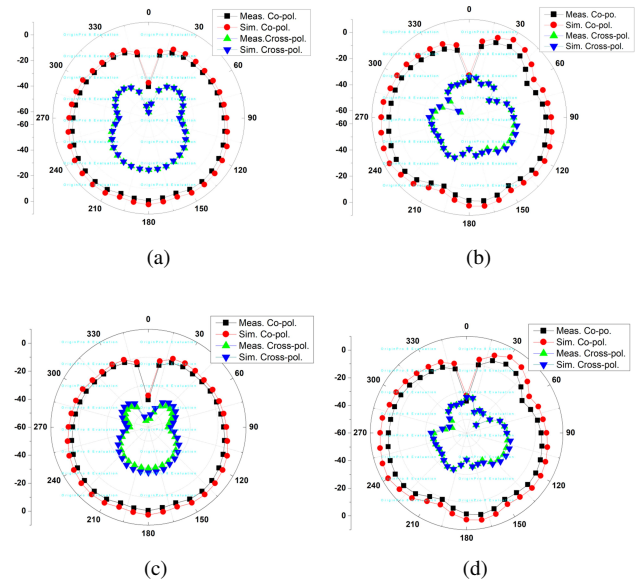


Fig. 11. (a), (c) XZ plane (or $\phi = 0^\circ$) and (b), (d) YZ plane (or $\phi = 90^\circ$) normalized radiation pattern at 27.10 GHz and 29.60 GHz, respectively.

References

- [1] FAN, Z., HAINES, R. Emerging technologies and research challenges for 5G wireless networks. *IEEE Wireless Communications*, 2014, vol. 21, no. 2, p. 106–112. DOI: 10.1109/MWC.2014.6812298
- [2] SHAFI, M., MOLISCH, A. F., SMITH, P. J., et al. 5G: A tutorial overview of standards, trials, challenges, deployment, and practice. *IEEE Journal on Selected Areas in Communications*, 2017, vol. 35, no. 6, p. 1201–1221. DOI: 10.1109/JSAC.2017.2692307
- [3] INTERNATIONAL TELECOMMUNICATIONS UNION (ITU). Studies on frequency-related matters for international mobile telecommunications identification including possible additional allocations to the mobile services on a primary basis in portion(s) of the frequency range between 24.25 and 86 GHz for the future development of international mobile telecommunications for 2020 and beyond. In *Proceeding of World Radiocommunication Conference (WRC-15)*. Geneva (Switzerland), 2015, p. 296–298.
- [4] QIAO, J., SHEN, X. S., MARK J. W., et al. Enabling device-to-device communications in millimeter-wave 5G cellular networks. *IEEE Communications Magazine*, 2015, vol. 53, no. 1, p. 209–215. DOI: 10.1109/MCOM.2015.7010536
- [5] RAPPAPORT, T. S., XING, Y., MACCARTNEY, G. R., et al. Overview of millimeter wave communications for fifth-generation (5G) wireless networks – with a focus on propagation models. *IEEE Transactions on Antennas and Propagation*, 2017, vol. 65, no. 12, p. 6213–6230. DOI: 10.1109/TAP.2017.2734243
- [6] BOZZI, M., GEORGIADIS, A., WU, K. Review of substrate integrated waveguide circuits and antennas. *IET Microwaves, Antennas & Propagation*, 2011, vol. 5, no. 8, p. 909–920. DOI: 10.1049/iet-map.2010.0463
- [7] TAGEMAN, O., LIGANDER, P., MANHOLM, L., et al. SIW antenna arrangement. *US Patent 9831565 B2*, Nov. 28, 2017.
- [8] AWIDA, M. H., SULEIMAN, S. H., FATHY, A. E. Substrate integrated cavity-backed patch arrays: A low-cost approach for bandwidth enhancement. *IEEE Transactions on Antennas and Propagation*, 2011, vol. 59, no. 4, p. 1155–1163. DOI: 10.1109/TAP.2011.2109681
- [9] ZAVOSH, F., ABERLE, J. T. Infinite phased arrays of cavity-backed patches. *IEEE Transactions on Antennas and Propagation*, 1994, vol. 42, no. 3, p. 390–398. DOI: 10.1109/8.280726
- [10] WU, K. Towards system-on-substrate approach for future millimeter-wave and photonic wireless applications. In *2006 Asia-Pacific Microwave Conference*. Yokohama (Japan), 2006, p. 1895–1900. DOI: 10.1109/APMC.2006.4429778
- [11] LI, Z., WU, K. 24-GHz frequency-modulation continuous-wave radar front-end system-on substrate. *IEEE Transactions on Microwave Theory and Techniques*, 2008, vol. 56, no. 2, p. 278–285. DOI: 10.1109/TMTT.2007.914363
- [12] ENTESARI, K., SAGHATI, A. P., SEKAR, V., et al. Tunable SIW structures: antennas, VCOs, and filters. *IEEE Microwave Magazine*, 2015, vol. 16, no. 5, p. 34–54. DOI: 10.1109/MMM.2015.2408273
- [13] LI, S., CAO, X., GAO, J. et al. High-isolation dual-polarized microstrip antenna via substrate integrated waveguide technology. *Radioengineering*, 2014, vol. 23, no. 4, p. 1092–1098. ISSN: 1210-2512
- [14] ABDEL-WAHAB, W. M., ABDALLAH, M., ANDERSON, J., et al. SIW-integrated parasitic DRA array: analysis, design, and measurement. *IEEE Antennas and Wireless Propagation Letters*, 2019, vol. 18, no. 1, p. 69–73. DOI: 10.1109/LAWP.2018.2880926
- [15] KUMAR, A., RAGHAVAN, S. Broadband SIW cavity-backed triangular-ring slotted antenna for Ku-band applications. *AEU: International Journal of Electronics*, 2018, vol. 87, p. 60–64. DOI: 10.1016/j.aeue.2018.02.016
- [16] CHOUBEY, P. N., HONG, W., HAO, Z., et al. A wideband dual-mode SIW cavity-backed triangular-complimentary-split-ring-slot (TCSRS) antenna. *IEEE Transactions on Antennas and Propagation*, 2016, vol. 64, no. 6, p. 2541–2545. DOI: 10.1109/TAP.2016.2550036
- [17] CASTELLANO, T., LOSITO, O., MESCIA, L., et al. Feasibility investigation of low cost substrate integrated waveguide (SIW) directional couplers. *Progress In Electromagnetics Research B*, 2014, vol. 59, p. 31–44. DOI: 10.2528/PIERB14010806
- [18] VENANZONI, G., MENCARELLI, D., MORINI, A., et al. Compact substrate integrated waveguide six-port directional coupler for X-band applications. *Microwave and Optical Technology Letters*, 2015, vol. 57, p. 2589–2592. DOI: 10.1002/mop.29388
- [19] VENANZONI, G., MENCARELLI, D., MORINI, A., et al. Compact double-layer substrate integrated waveguide magic tee for X-band applications. *Microwave and Optical Technology Letters*, 2016, vol. 58, p. 932–936. DOI: 10.1002/mop.29707
- [20] XU, F., WU, K. Guided-wave and leakage characteristics of substrate integrated waveguide. *IEEE Transactions on Microwave Theory and Techniques*, 2005, vol. 53, no. 1, p. 66–73. DOI: 10.1109/TMTT.2004.839303
- [21] AWIDA, M. H., FATHY, A. E. Design guidelines of substrate integrated cavity backed patch antennas. *IET Microwaves, Antennas & Propagation*, 2012, vol. 6, no. 2, p. 151–157. DOI: 10.1049/iet-map.2011.0376
- [22] DESLANDES, D., WU, K. Design consideration and performance analysis of substrate integrated waveguide components. In *2002 32nd European Microwave Conference*. Milan (Italy), 2002, p. 1–4. DOI: 10.1109/EUMA.2002.339426
- [23] RAYAS-SANCHEZ, J. E., GUTIERREZ-AYALA, V. A general EM-based design procedure for single-layer substrate integrated waveguide interconnects with microstrip transitions. In *2008 IEEE MTT-S International Microwave Symposium Digest*. Atlanta (USA), 2008, p. 983–986. DOI: 10.1109/MWSYM.2008.4632999
- [24] ARORA, R., RANA, S. B., ARYA, S. Performance analysis of Wi-Fi shaped SIW antennas. *AEU: International Journal of Electronics*, 2018, vol. 94, p. 168–178. DOI: 10.1016/j.aeue.2018.07.002
- [25] KHALID, M., NAQVI, S. I., HUSSAIN, N., et al. 4-port MIMO antenna with defected ground structure for 5G millimeter wave applications. *Electronics*, 2020, vol. 9, p. 1–13. DOI: 10.3390/electronics9010071
- [26] SHARMA, S., KANAUIA, B. K., KHANDELWAL, M. K. Analysis and design of single and dual element bowtie microstrip antenna embedded with planar long wire for 5G wireless applications. *Microwave and Optical Technology Letters*, 2020, vol. 62, p. 1281–1290. DOI: 10.1002/mop.32137
- [27] BISWAL, S. P., SHARMA, S. K., DAS, S. Circularly polarized 5G band MIMO antenna array for future user terminals. In *2020 International Applied Computational Electromagnetics Society Symposium (ACES)*. Monterey (USA), 2020, p. 1–2. DOI: 10.23919/ACES49320.2020.9196170
- [28] WANI, Z., ABEGAONKAR, M. P., KOUL, S. K. A 28-GHz antenna for 5G MIMO applications. *Progress In Electromagnetics Research Letters*, 2018, vol. 78, p. 73–79. DOI: 10.2528/PIERL18070303
- [29] YASHCHYSHYN, Y., DERZAKOWSKI, K., BOGDAN, G., et al. 28 GHz switched-beam antenna based on S-PIN diodes for 5G mobile communications. *IEEE Antennas and Wireless Propagation Letters*, 2018, vol. 17, no. 2, p. 225–228. DOI: 10.1109/LAWP.2017.2781262
- [30] GHARBI, I., BARRAK, R., DIALLO, A., et al. Investigation of stacked balanced-fed patch antenna for millimeter-wave application. *Radioengineering*, 2020, vol. 29, no. 3, p. 452–459. DOI: 10.13164/re.2020.0452

- [31] HAN, W., YANG, F., OUYANG, J., et al. Low-cost wideband and high-gain slotted cavity antenna using high-order modes for millimeter-wave application. *IEEE Transactions on Antennas and Propagation*, 2015, vol. 63, no. 11, p. 4624–4631. DOI: 10.1109/TAP.2015.2473658

About the Authors . . .

Amit KUMAR was born in Agra, Uttar Pradesh, India, in 1993. He received his B.Tech degree in Electronics and Communication Engineering from Ambedkar Institute of Advanced Communication Technologies and Research, affiliated to Guru Gobind Singh Indraprastha University (GGSIPU), India, in 2014 and masters in Electronics and Communication (ECE) from University School of Information, Communication and Technology (USIC&T), Guru Gobind Singh Indraprastha University (GGSIPU), India, in 2016. He is currently pursuing his Ph.D. from IIT (BHU), Varanasi, India. His research interests include SIW-based antennas and circuits, broadband antennas, circularly polarized antennas MMW and THz bands.

Munish KUMAR was born in New Delhi, India, in 1990. He received his M. Tech in ECE from USIC&T, GGSIPU, India, in 2015. He is currently pursuing his Ph.D. degree from USIC&T, GGSIPU, New Delhi, India. He has worked extensively and authored more than 20 research articles on multiband and wideband microstrip patch antennas, fractals, electromagnetic bandgap structures (EBG), circularly polarized and MIMO antennas in various international journals and conferences. His current research involves designing of microstrip antennas for wideband and multiband applications.

Amit Kumar SINGH (corresponding author) received the Ph.D. degree from the IIT (BHU) Varanasi in 2010 respectively. He was working as Associate Professor in the Electronics Engineering department in IIT (BHU) since 2012. His research interest includes the areas of design of millimeter frequency antennas, feeds for parabolic reflectors, dielectric resonator antennas, microstrip antennas, EBG, artificial magnetic conductors, soft and hard surfaces, Antennas for RFIDs, phased array antennas, and computer aided design for antennas. He has published and co-authored over 70 journal articles and conference articles.